Cellulose–Copolyamide 6,69 Blends

M. GARCIA-RAMIREZ,* J. Y. CAVAILLE, A. DUFRESNE,† and D. DUPEYRE

Centre de Recherches sur les Macromolécules Végétales (CERMAV-CNRS), Université Joseph Fourier, B.P. 53, F-38041 Grenoble Cedex 9, France

SYNOPSIS

In a previous work [*J. Polym. Sci. Polym. Phys.*, **32**, 1437 (1994)], a technique for the preparation of cellulose–polyamide 66 (PA66) blends was proposed. It was shown that the crystallization of PA66 is responsible for the phase separation and, furthermore, for the morphology of the domains in the blends. For this reason, the use of a quasi-amorphous polyamide, i.e., a random copolymer of units 6 nd 69, instead of PA66, is now investigated. Cellulose–polyamide 669 (PA669) blends were prepared by a solution–precipitation process. A mixture of *N*-methylmorpholine-*N*-oxide and phenol (80/20 wt/wt) was used as a common solvent. Materials were precipitated whether in methanol or in water. The fibers obtained were characterized by scanning electron microscopy, mechanical spectroscopy, and tensile tests. It is shown that the morphology of these blends depends on the precipitation system and is a function of the different steps of processing of the blends. © 1996 John Wiley & Sons, Inc.

INTRODUCTION

In quite recent years, blends with cellulose and synthetic polymers have been studied more and more. The interest of these blends is, on the one hand, the use of an abundant naturally occurring polymer, namely, cellulose, and, on the other hand, the possibility to have favorable intermolecular interactions, like hydrogen bonds, between this natural polymer and some synthetic polymers. The presence of functional groups in these synthetic polymers could allow the interactions with the hydroxyl groups of cellulose. Actually, several synthetic polymers have been blended with cellulose such as poly(vinyl alcohol),[1–5] polyacrylonitrile,[5–9] poly(ethylene oxide),[10] nylon 6,[5,11] and polyamide 66.[12–15] These blends were prepared using different solvents like dimethyl sulfoxide/paraformaldehyde (DMSO/PF),[3,7] *N*,*N*-dimethylacetamide/lithium chloride (DMAc–LiCl),[1,2,5,8–11] and *N*-methylmorpholine-*N*-oxide (NMMO).[12–15] Recently, we showed that it is possible to prepare blends of cellulose with polyamide 66 (PA66) using a mixture of NMMO and phenol as a common solvent.[15] We observed a partial miscibility between both polymers.[16] In the present work, we extended the study of this kind of blends to the cellulose/copolyamide 6,69 (PA669) system. This copolyamide is a random copolymer (50/50 wt/wt) of units 6 and units 6,9. In the case of cellulose/PA66 blends, we observed that the phase separation of these polymers occurs during the crystallization of PA66, when PA66 and the cellulose solutions are mixed together. Since PA669 is mainly amorphous, it is interesting to verify if a partial miscibility occurs in this system. Cellulose/PA669 blends were prepared by a solution–coagulation method using NMMO as a solvent and they were precipitated in water or in methanol. The materials were characterized by scanning electron microscopy (SEM) and mechanical spectroscopy.

EXPERIMENTAL

Raw Materials

PA669 was kindly supplied by Dr. Moshé Narkis of Technion, Israel. This polyamide is a random copolymer (50/50 wt/wt) of units 6 and units 6,9. It

* Present address: Industriales NEGROMEX S. A. DECIV Investigacion y Desarollo, KM 28.5 Carretera Mante, 280 TAMPICO ALTAMIRA.

† To whom correspondence should be addressed.

Journal of Applied Polymer Science, Vol. 59, 1995–2007 (1996)

CCC 0021-8995/96/131995-13

was dried under vacuum and kept in a dessicator over phosphorus pentoxide (P_2O_5) until used. Cellulose (V60) was supplied by Buckeye Cellulose Corp. (U.K.). The average degree of polymerization ($\overline{DP}$) was 600. Its purity has been checked and its glucose content was found to be around 97%. Solvents used were *N*-methylmorpholine-*N*-oxide (NMMO) and phenol purchased from Texaco (U.S.A.) and Prolabo (France), respectively. Propyl gallate purchased from Fluka (France) was used as an antioxidant agent to avoid as much as possible the degradation of polymers.

Preparation of Samples

All materials were prepared following the procedure described elsewhere.[15] In this case, the common solvent used for both polymers was a mixture of monohydrate NMMO (referred as NMMO, H_2O) and phenol in a ratio 80/20 (wt/wt). A cellulose solution was prepared as described in Ref. 15. As-received pellets of PA669 were first milled in the presence of liquid N_2 to obtain a powder with an average grain size of 50 μm. Phenol and NMMO, H_2O were mixed and then the powder of PA669 was dissolved at 120°C under mechanical stirring for 20 min. The total amount of the polymer was 5 wt % (see Table I). The homopolymer solutions were prepared in the presence of 0.1 wt % of propyl gallate as the antioxidant. Both solutions were mixed in a small mixer (Mini-max Model CS-183 mmx, from Custom Scientific Instruments, U.S.A.) in appropriate ratios to produce blends with final compositions of 100/0, 80/20, 65/35, and 50/50 (wt/wt), the first number referring to cellulose throughout this work. To obtain fibers with an average diameter of 0.6 mm, the different mixtures were then poured into an injection spinning device[17,18] fitted with a 2 mm-diameter die. The mixture was extruded at 60°C (333 K). The fibers were precipitated in water because it is a good solvent for NMMO and phenol but not one at all for these polymers. To determine if the coagulation system can play any role on the properties of the materials, the fibers were also precipitated in methanol, which is a good solvent for NMMO and phenol, a poor one for PA669, but not one at all for cellulose. Each sample tested has a constant diameter close to 0.6 mm along its length within ±0.01 mm. Finally, all samples were dried at room temperature under a vacuum and stored in a dessicator until used. Mass spectrometry (NERMAG R1010C) was used to confirm the absence of solvents in the materials.

Measurements

A scanning electron microscope (SEM) from JEOL (JSM-6100) was used for studying the morphology of the materials. The fibers were fractured and observed as already described.[15] Dynamic mechanical measurements were performed with a mechanical spectrometer described elsewhere[19,20] and commercially available at Metravib RDS (Ecully, France). It consists of a forced oscillation pendulum working in the temperature range 100–700 K and in the frequency range 10^{-5} to 5 Hz. It provides the storage (G') and loss (G'') moduli of the complex shear modulus (G^*) and the internal friction coefficient tan $\phi(G''/G')$ as a function of frequency (isothermal conditions) or temperature (isochronal conditions). The accuracy of tan ϕ is better than 5×10^{-4}, while for the relative change of G', it is better than 10^{-3}. To remove most of water from the material, the fibers were immediately heat-treated *in situ* in the spectrometer at 400 K for 1 h under a vacuum before any measurement. It was checked that in these conditions the behavior is not modified by a further heat treatment. Measurements were performed from 100 to 400 K at three frequencies, i.e., 0.01, 0.1, and 1 Hz, in the presence of liquid nitrogen. Between the two measurements, the temperature was increased by 1 K and the average temperature rate was 12 K/h.

The nonlinear mechanical behavior was analyzed using an Instron 4301 testing machine (U.K.) in the tensile mode, with a load cell of 100 N capacity. Tensile tests were performed at a strain rate $\dot{\varepsilon} = 1.7$

Table I Composition and Codification of the Samples

Sample	Cellulose (Wt %)	PA669 (Wt %)	Anhydre NMMO (Wt %)	Phenol (Wt %)	Water (Wt %)
100/0	5	0	66	19	10
80/20	4	1	66	19	10
65/35	3.25	1.75	66	19	10
50/50	2.5	2.5	66	19	10

$\times 10^{-3}$ s^{-1} and at room temperature. For each measurement, it was checked that the strain was uniform along the sample, until its break. So, the strain ε can be determined by $\varepsilon = \ln(l/l_0)$, where l and l_0 are the length during the test and the length at zero time, respectively. The stress σ is calculated by $\sigma = F/S$, where F is the applied strength, and S, the cross-section. S is determined assuming that the total volume of the sample remains constant, so that $S = S_0 \cdot l_0/l$, where S_0 is the cross section at zero time. Thus, the additional error $\delta\sigma/\sigma$, due to this simplification is smaller than 2% for strain smaller than 10%.

Morphology of Samples

The homopolymer solutions were all optically clear. When cellulose and PA669 solutions are mixed, a phase segregation occurs. On account of the weak contrast of polymer solutions, it was not possible to take an optical micrograph. The polyamide solution forms domains on the cellulose solutions for any composition. Polyamide domains have a very broad size distribution and are irregularly dispersed. Their shape can be modified during the processing of blends (extrusion, casting, etc.).

The observations by SEM were made following the method described elsewhere.[15] Figure 1 shows the surface of fibers just after the fracture for all the blends precipitated in water. By comparing the micrographs showing the surface of fracture of pure cellulose fiber and of the blends, it is easy to identify PA669 domains. In fact, polyamide domains appear like "marbles" or beads, whose size and distribution are very irregular. Their concentration is a direct function of the polyamide composition in the blends. These beads are embedded in cellulose and the adhesion between both polymer domains appears to be very weak, as displayed by the space located in the interphase region. Figure 2 shows the surface of

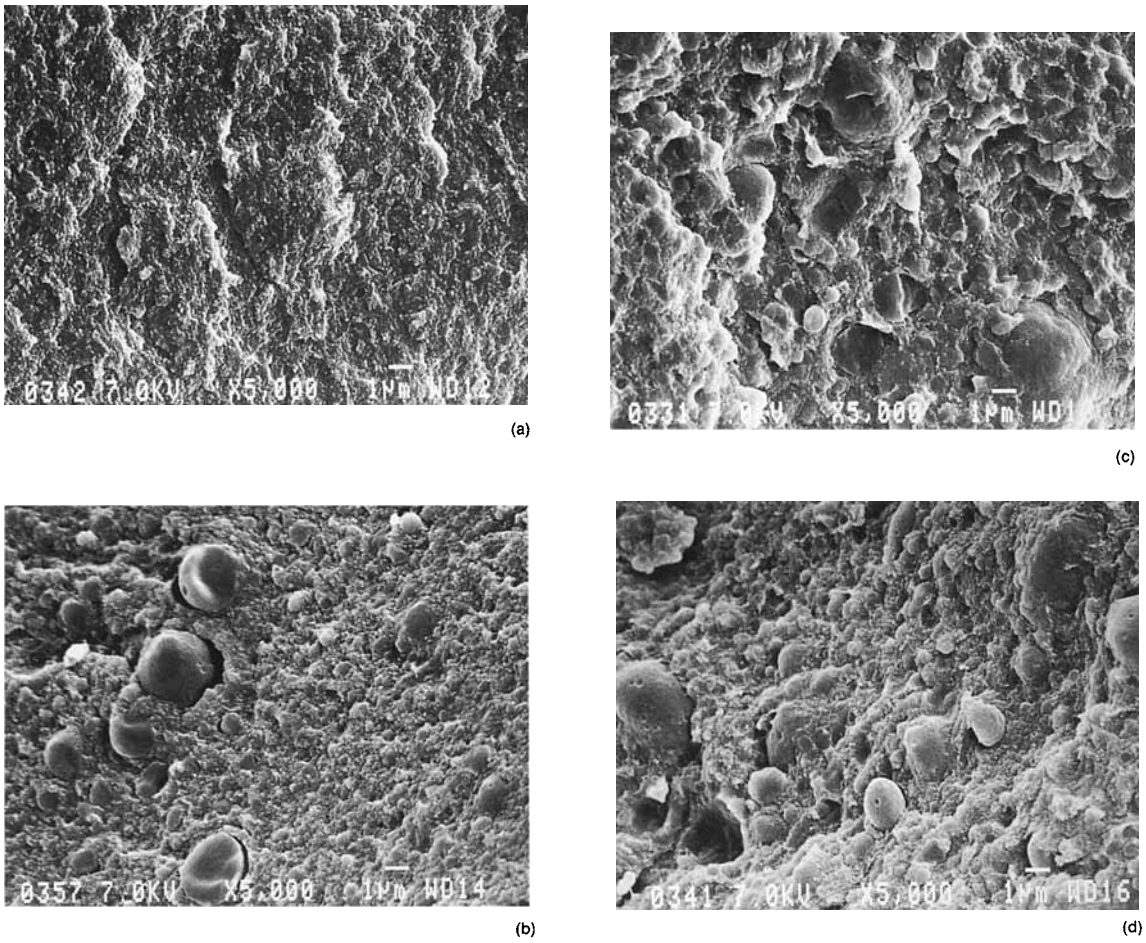

Figure 1 Scanning electron micrographs showing the fractured surfaces of (a) pure cellulose, (b) 80/20, (c) 65/35, and (d) 50/50 blends precipitated in water.

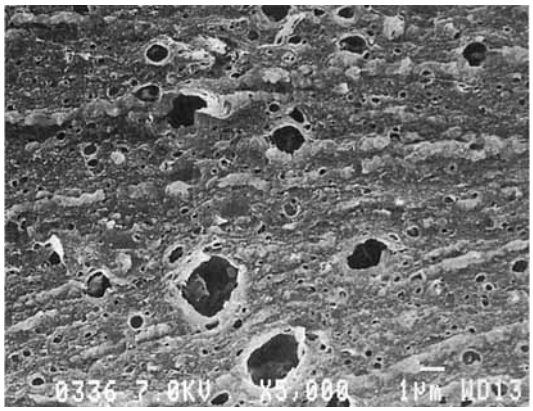

(a)

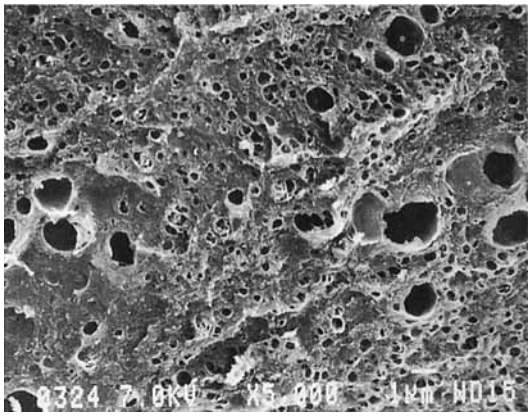

(b)

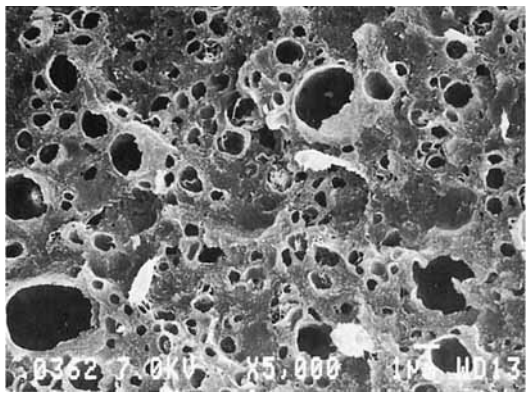

(c)

Figure 2 Scanning electron micrographs showing the fractured surfaces of (a) 80/20, (b) 65/35, and (c) 50/50 blends precipitated in water, after etching by phenol.

the fracture for the different blends after etching by phenol. In these micrographs, the presence of holes can be observed. The size and dispersion of these holes correspond to those already observed for the "marbles" in Figure 1. It is clear that they correspond to the polyamide domains which have been removed from the fibers by phenol. Contrarily to the blends, pure cellulose is not modified by this solvent. This is an indication that cellulose and polyamide 669 form mainly a two-phase system, in which the continuous phase is formed by cellulose and the inclusions (bead-shaped) are PA669 domains.

The surface of fracture of the fibers precipitated in methanol are shown in Figure 3. In this case, it is also possible to distinguish the polyamide domains from the comparison between pure cellulose and the blends. Polyamide domains appear darker and smoother on the surface. The presence of cracks can also be observed in the interphase zone between the cellulose and polyamide, but they are smaller than in the case of materials precipitated in water. The cohesion of these materials seems to be better compared to those precipitated in water. Figure 4 shows the surface of fracture of different blends after etching. From the comparison between Figures 3 and 4, evidence of the phase separation is given by the presence of holes which correspond also to the dissolution of PA669 by phenol. The PA669 domains seem to be larger when methanol is used as a coagulation solvent, as displayed in Figure 4(b) or (c). Moreover, these results indicate that the continuous phase is formed mainly by cellulose.

For both kinds of material, the loss of weight of polyamide in the presence of phenol was measured as a function of the time during 1 week ($\approx 10^6$ s). Results are reported in Figure 5. For all the materials, the kinetic of loss of weight is very slow, but most of the polyamide is removed from the fibers precipitated in water after 1 week. On the contrary, for the materials precipitated in methanol, PA669 does not seem to be removed from the fibers. In the case of the 80/20 blend, a slight loss of weight is observed after 1 week. However, in the blends, polyamide is never completely removed. This could be explained by the fact that this fraction of polyamide ($\approx$ 15%) stays in the fibers or, alternatively, that this fraction has been lost during the precipitation step of materials, due to the partial dissolution of polyamide in methanol.

Dynamic Mechanical Properties

Dynamic mechanical properties were performed on pure cellulose, pure PA669, and different blends precipitated whether in water or in methanol. The curves corresponding to 0.01, 0.1, and 1 Hz are presented only for pure cellulose (100/0 sample) using water as the coagulation system and pure PA669 in

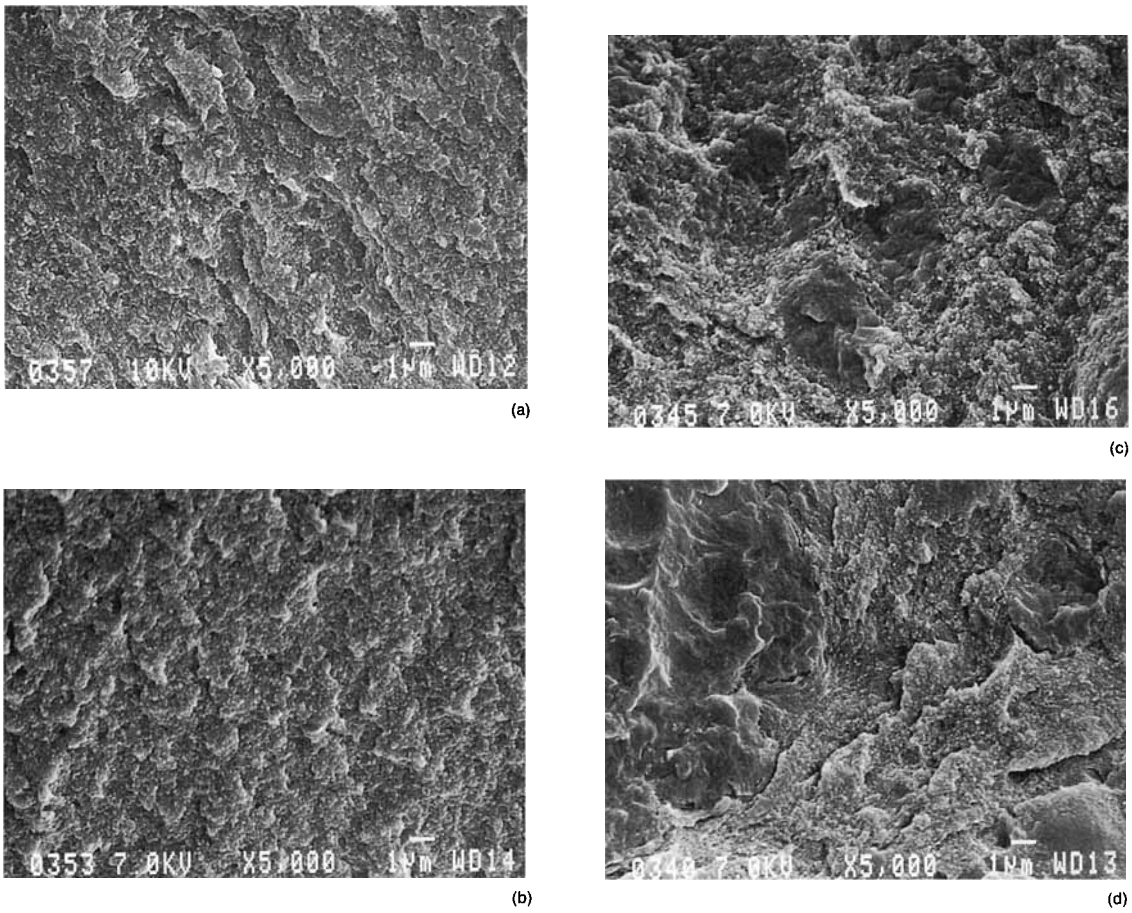

Figure 3 Scanning electron micrographs showing the fractured surfaces of (a) pure cellulose, (b) 80/20, (c) 65/35, and (d) 50/50 blends precipitated in methanol.

Figure 6. Pure cellulose displays two relaxation processes in the temperature range 100–400 K. Since its glass–rubber transition and its main relaxation or α process cannot be reached without its degradation, we propose to call these two secondary relaxations β and γ. At 0.1 Hz, tan ϕ passes through a maximum at 215 and 150 K. The β relaxation is generally associated to cooperative motions of segments of the main chain, which involve the flexibility of the glycosidic bonds $\beta(1 \rightarrow 4)$, while the γ relaxation should correspond to the rotation of the primary hydroxyl groups linked to the lateral units CH_2OH.[21] Pure PA669 exhibits three relaxation processes, referred to as α, β, and γ, as temperature decreases. At 0.1 Hz, tan ϕ passes through a maximum at 300, 185, and 120 K. From these isochronal measurements, it is possible to determine the apparent activation energy ΔE and the preexponential factor f_0 associated to each relaxation process, assuming an Arrhenius behavior. The results are listed in Table II. The activation energy corresponding to the α relaxation process is much higher than that of the others. Therefore, the main relaxation α is attributed to the inelastic manifestation of the glass–rubber transition, which leads to the elastic modulus drop of about one decade in the temperature range 250–330 K. The mechanism of the α relaxation involves cooperative motions of long-chain sequences. The β relaxation at 185 K is known to correspond to motions of water molecules linked by hydrogen bonds to CO and/or NH groups. As for the γ relaxation, it is often associated to the local motions of short aliphatic sequences, described as the result of

Table II Apparent Activation Energies of PA669

Relaxation	γ	β	α
ΔE (kJ/mol)	36	70	353
f_0 (Hz)	10^{15}	10^{18}	10^{60}

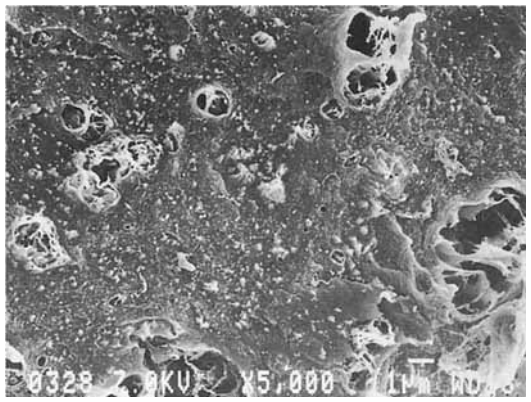

(a)

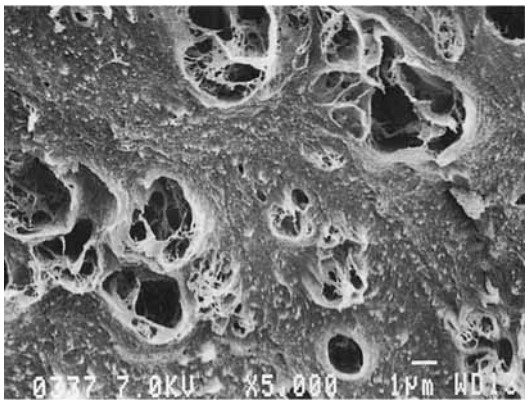

(b)

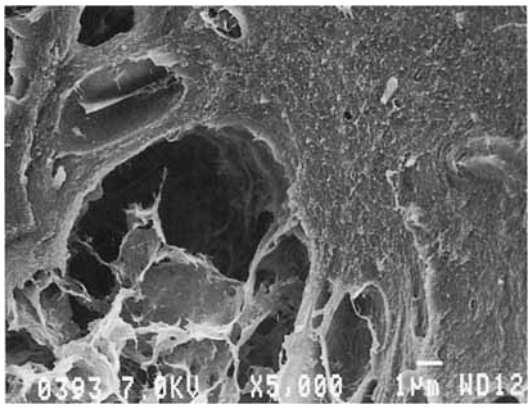

(c)

Figure 4 Scanning electron micrographs showing the fractured surfaces of (a) 80/20, (b) 65/35, and (c) 50/50 blends precipitated in methanol, after etching by phenol.

the "crank shaft" of the aliphatic segments of the chain.[22,23]

Figure 7 exhibits the evolution of log(G') and log(tan ϕ) at 0.1 Hz as a function of temperature for the other materials precipitated in water. The same behavior for the blends precipitated in methanol is reported in Figure 8. To compare the mechanical behavior for each blend and for the sake of clarity, each curve was shifted by one decade with regard to the previous one, pure cellulose being the reference.

All the blends exhibit two secondary relaxation processes broader than in homopolymers, which result from the superposition of the secondary relaxations of the two homopolymers. All the temperature positions of the various relaxation processes are reported in Table III. It is interesting to observe that the γ relaxation of pure cellulose and pure PA669 occurs in the same temperature range, 120 K for PA669 and around 150 K for cellulose, for any coagulation system. However, the peak associated to the γ relaxation in blends is located at higher temperature for the materials precipitated in methanol. The β relaxation of cellulose appears at a temperature between those of the β and α relaxations of PA669. It is worthy to note that the β relaxation temperature also depends on the coagulation system.

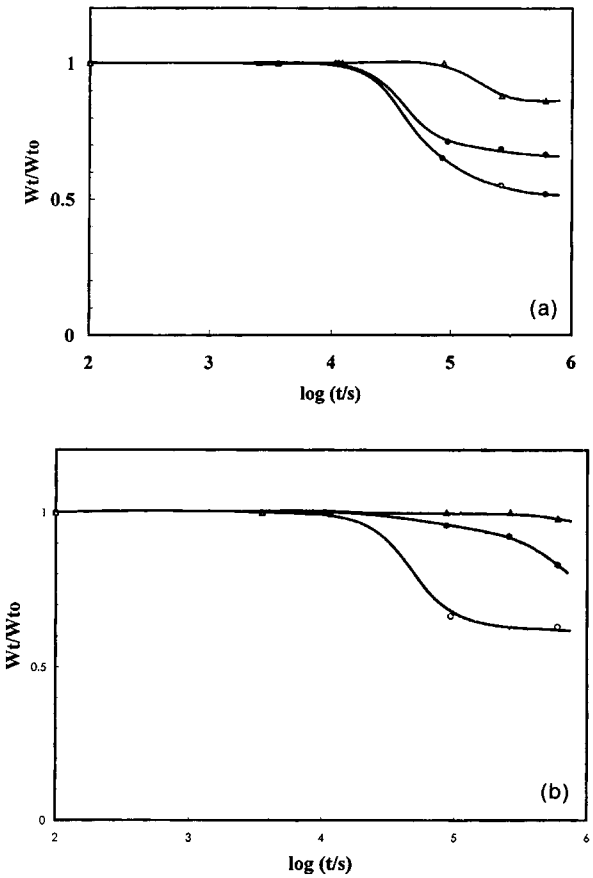

Figure 5 Loss of weight of polyamide in the presence of phenol vs. time for (○) 50/50, (●) 65/35, and (△) 80/20 blends precipitated (a) in water and (b) in methanol.

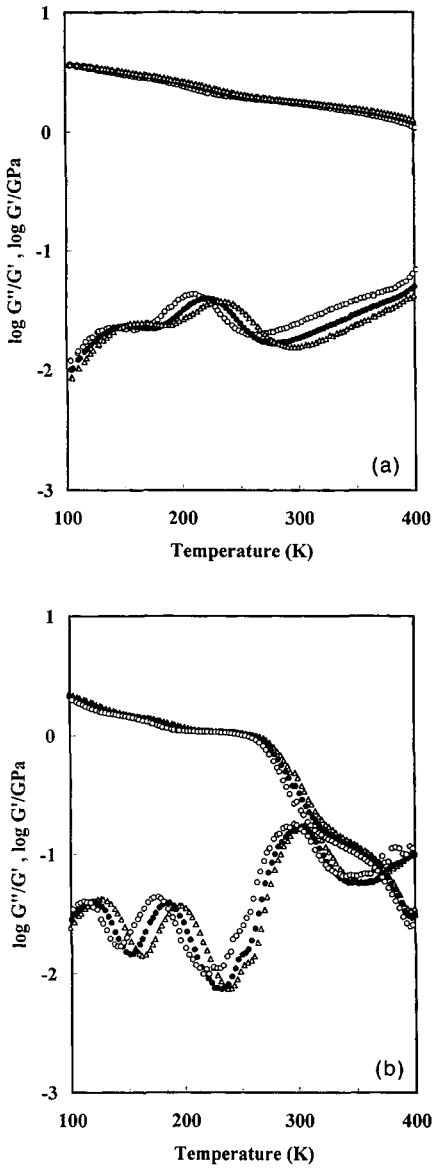

Figure 6 The storage shear modulus (G') and the internal friction coefficient (tan ϕ) vs. temperature at (○) 0.01 Hz, (●) 0.1 Hz, and (△) 1 Hz for (a) pure cellulose and (b) pure PA669.

Indeed, it appears at 215 and 222 K for cellulose precipitated in water and in methanol, respectively. It is surprising to observe that the β relaxation is located at higher temperatures the higher the polyamide content is.

In the temperature range 250–400 K, cellulose does not exhibit any relaxation process, whereas the α relaxation of PA669 appears. This relaxation mechanism is also observed in the blends. The presence of PA669 in the materials can be then characterized by its main relaxation. As a matter of fact, for all the materials precipitated in water, tan ϕ passes through a maximum at 313, 308, and 305 K, and for the materials precipitated in methanol, at 320, 317, and 318 K, for the 50/50, 65/35, and 80/20 blends, respectively. The drop of the elastic modulus G' in the temperature range 290–320 K is more significant the higher the polyamide content is. Moreover, it is noteworthy that for all the compositions the α relaxation maximum is shifted toward

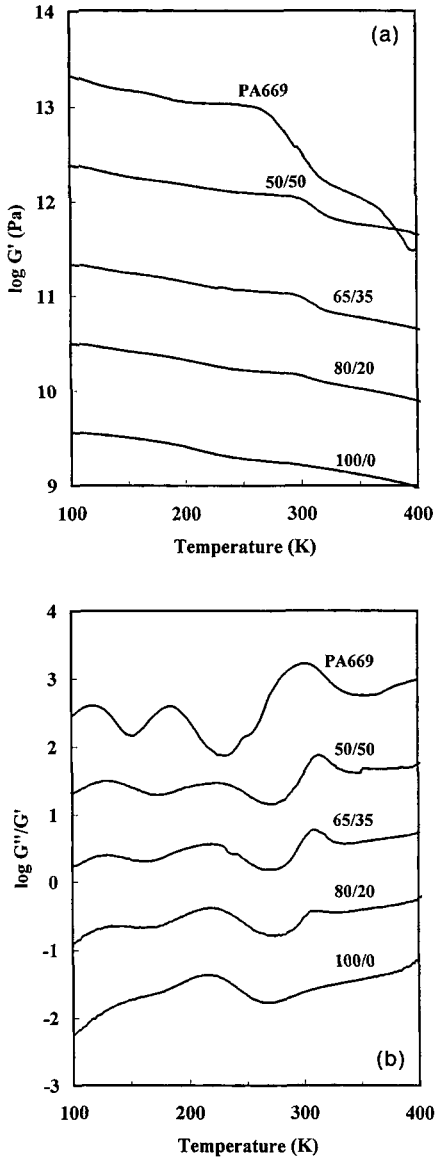

Figure 7 (a) The storage shear modulus (G') and (b) the internal friction coefficient (tan ϕ) vs. temperature at 0.1 Hz for blends 100/0 (pure cellulose) to pure PA669 precipitated in water. Scales correspond to curves 100/0. Each other curve (80/20 to pure PA669) is shifted by one decade for the sake of clarity.

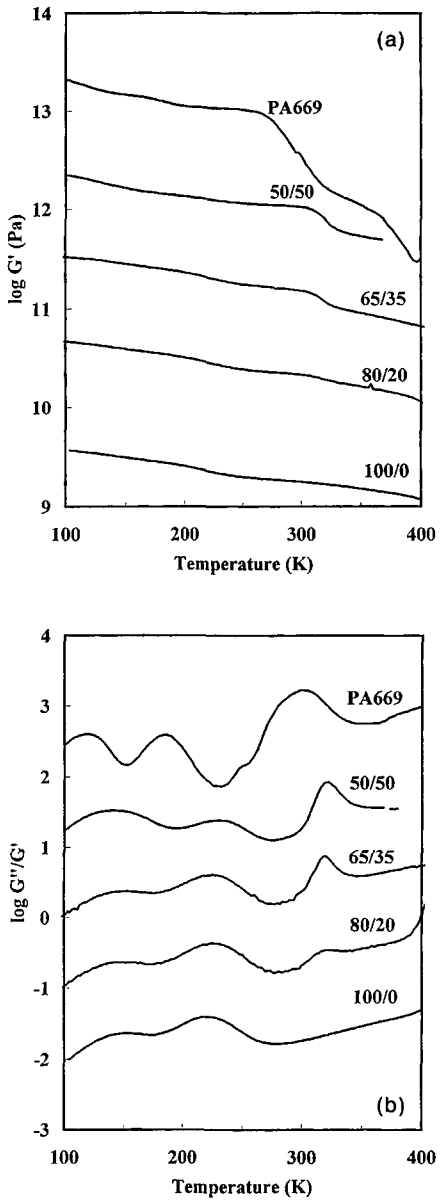

Figure 8 (a) The storage shear modulus (G') and (b) the internal friction coefficient (tan ϕ) vs. temperature at 0.1 Hz for blends 100/0 (pure cellulose) to pure PA669 precipitated in methanol. Scales correspond to curves 100/0. Each other curve (80/20 to pure PA669) is shifted by one decade for the sake of clarity.

higher temperatures with respect to pure PA669. The extent of this shift ranges between 5 and 13 K using water as the coagulation system and between 17 and 20 K for materials precipitated in methanol.

DISCUSSION

PA669 domains can be distinguished on the surface of fracture of fibers for all the blends. They have been determined by SEM observations. These domains have a broad size distribution and they are irregularly dispersed. Contrarily to the observations made on cellulose/PA66 blends,[15] the size and spatial distribution of PA669 domains are modified during the different steps of the processing of the blends. The morphology of these domains depends greatly on the coagulation system. From the optical observations, it seems that the phase separation of the cellulose/PA669 blends begins when the solutions of parent polymers are mixed.

Since phenol removes PA669 from the fibers, it confirms that cellulose and PA669 form mainly a two-phase system. In the case of materials precipitated in water, most of PA669 is removed by phenol. On the other hand, for the materials precipitated in methanol, the loss of weight of polyamide corresponds only to 85% of the weight at the beginning. It could be explained in terms of the dissolution of PA669 by methanol during the precipitation step which could modify the initial composition of the blends or in terms of a partial miscibility between both polymers. In this latter case, it is thus possible that a fraction of polyamide is mixed with cellulose in such a way that PA669 could not be dissolved any more by phenol.

To determine a possible miscibility between cellulose and PA669, we also analyzed the dynamic mechanical properties of these blends. It is especially of interest to predict the mechanical behavior of the materials. Different models can be used to predict the elastic behavior of two-phase systems such as blends of amorphous polymers.[24-30] In this work, we considered a series-parallel model as proposed by Takayanagi[25] in which the concept of percolation was introduced.[30] This is a phenomenological model, which consists of a mixing rule between the two lim-

Table III Temperature for the Various Relaxation Processes: α (T_α), β (T_β), and γ (T_γ), for the Blends Precipitated Either in Water or in Methanol

Coagulation System	Material	T_γ	T_β	T_α
	PA669	120	185	300
Water	50/50	130	222	312
	65/35	129	218	308
	80/20	133	218	305
	100/0	150	215	—
Methanol	50/50	141	230	320
	65/35	148	224	317
	80/20	144	225	318
	100/0	149	222	—

its of the series model (Reuss) and of the parallel model (Voigt). A schematic diagram is reported in Figure 9, where R and S refer to rigid and soft phases, respectively. λ and ψ are the parameters of this mixing rule and $v_s = \lambda(1 - \psi)$ is the volume fraction of the soft phase. For a rigid matrix/soft inclusions system, $v_s = 1 - v_r$ (v_r being the volume fraction of phase R). ψ is the volume fraction of the rigid phase which has percolated,[30] i.e., which really reinforces the material. With v_{rc} being the critical volume fraction of the rigid phase at the percolation threshold, and b, the corresponding critical exponent, ψ can be written as $\psi \approx A(v_r - v_{rc})^b$ for $v_r > v_{rc}$ and $\psi = 0$ for $v_r < vrc$. To be consistent with the fact that ψ should be equal to 1 when $v_r = 1$,

$$\psi = v_r\left[\frac{v_r - v_{rc}}{1 - v_{rc}}\right]^b \tag{1}$$

and the shear modulus becomes

$$\frac{G}{G_r} = \frac{(1 - \psi - \psi v_s)G_s + \psi v_s G_r}{(1 - \psi - v_s)G_s + v_s G_r} \tag{2}$$

Furthermore, the behavior of polymers is not purely elastic, but, in fact, viscoelastic.[31] For this reason, it is usual to modify the relationships for elasticity in introducing viscoelastic moduli (for each phase), i.e., under their complex form $G^*(i\omega, T)$.[27,32] The viscoelastic behavior is obtained using the complex shear modulus G_s^* for the soft phase and G_r^* for the rigid phase as described elsewhere.[16]

$$\frac{G^*}{G_r^*} = \frac{(1 - \psi - \psi v_s)G_s^* + \psi v_s G_r^*}{(1 - \psi - v_s)G_s^* + v_s G_r^*} \tag{3}$$

Though it is difficult to determine v_{rc} and b [eq. (1)] as they depend on many parameters such as the geometry and spatial distribution of each phase, we considered that $v_{rc} = 1 - v_{max}$, where v_{max} is the maximum volume fraction of rigid isoradius spheres, so that $v_{Rc} \approx 0.25$. The critical exponent of the probability to obtain an infinite cluster is about 0.4 for the random sites percolation model.[33,34] This model requires the knowledge of the experimental mechanical behavior of the pure parent components: cellulose and PA669. It is worthy to note that the cellulose mechanical behavior depends on the coagulation system used during the processing.

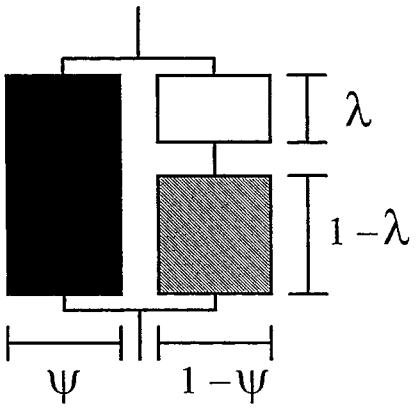

Figure 9 Schematic diagram for the series-parallel coupling model.

In this work, calculations were performed at 0.1 Hz for all the blends. Such calculated curves are shown in Figures 10 and 11 for the blends precipitated in water and in methanol, respectively, as well as the experimental data.

We ascertain that the experimental data are in good agreement with the theoretical ones in the β relaxation zone for blends precipitated in water (Fig. 10), except for the higher polyamide content material, i.e., for the 50/50 blend. For this latter sample, the experimental β relaxation is truncated in the low-temperature side, with respect to the theoretical one. It seems that the PA contribution to this relaxation process is partially excluded. This effect could originate from the fact that cellulose is more hydrophilic than is PA, due to the more significant concentration of hydroxyl groups. The water molecules which remain in the blend after the heat treatment and during the experiment tend to largely diffuse throughout the material toward the cellulose domains. The magnitude of the β relaxation in PA is therefore lowered. This effect is all the more significant the higher is the PA content in the blend. The γ relaxation process is well predicted from the model with regard to its temperature position. On the other hand, the magnitude of the experimental γ relaxation is always higher than the predicted one. However, we note that the model is globally consistent with the experimental behavior of the materials precipitated in water in the low-temperature zone. The good agreement in the secondary relaxation zone between the model and the experimental curves for the blends precipitated in water is probably the sign of weak interactions between the two parent polymers.

On the contrary, the stronger modifications of the characteristics of these relaxations in the case of blends precipitated in methanol should result from interactions at the molecular level between PA669 and cellulose. In the secondary relaxation zone, it appears that the molecular motions responsible for these relaxation processes are more constricted, as displayed by the shift toward higher

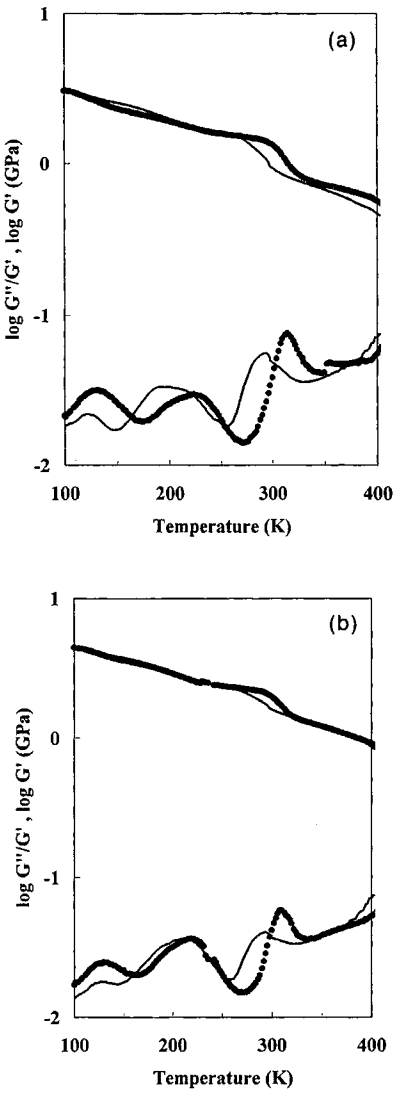

Figure 10 (●) Experimental thermograms and (——) calculated thermograms from the percolation model for the dynamic mechanical behavior at 0.1 Hz of (a) 50/50, (b) 65/35, and (c) 80/20 blends precipitated in water.

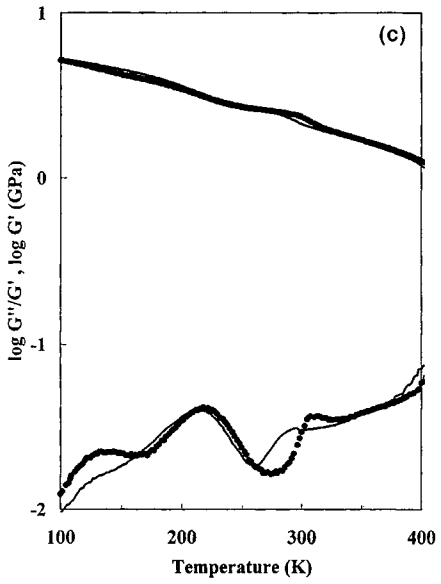

Figure 10 (*Continued*)

temperature. This phenomenon is probably due in part to the preferential localization of water molecules in the cellulose domains, as in the case of blends precipitated in water. Moreover, the weight loss experiments have shown that a fraction of polyamide is dissolved in methanol during the precipitation step.

In fact, no direct conclusion can be obtained in the secondary relaxation temperature range. On the contrary, the evolution of the α tan ϕ peak is of major interest, because it can display potential miscibility phenomena. We ascertain in Figures 7 and 8 that the temperature of the α tan ϕ peak is about 10 K higher for the blends precipitated in water and 20 K using methanol as the coagulation system than for pure PA669. This shift of the α tan ϕ peak toward higher temperature could originate from various effects: (i) a mechanical coupling between phases related to the phase morphology, and (ii) an increase of the glass transition temperature of PA669, both due to its partial miscibility with cellulose. Moreover, we ascertain that the magnitude of the storage modulus drop associated to the α relaxation is slightly lower for the blends precipitated in methanol. This confirms that a fraction of polyamide is dissolved in methanol during the precipitation step, as indicated by the weight loss experiments. By comparing the experimental isochronal curves of the various blends in the α relaxation range with predicted data using the percolation model, we ascertain that the model fails to describe the experimental behavior. Indeed, we note that (i) the loss angle peak is broader for the experimental curves than for the calculated ones, and (ii) the experimental tan ϕ peak is located at higher temperature, as well as the storage modulus drop, with respect to the calculated ones. The temperature shift is about 10 K using water as the coagulation system and 20 K with methanol, i.e., the same as those experimentally observed between pure PA669 and blends. In Figure 12, the calculated and experimental values of the temperature at the maximum of the internal friction coefficient ($T_{G''/G'}$) are reported as a function of PA669 content in all the blends for the different coagulation systems. It is worthy to note that in the case of the

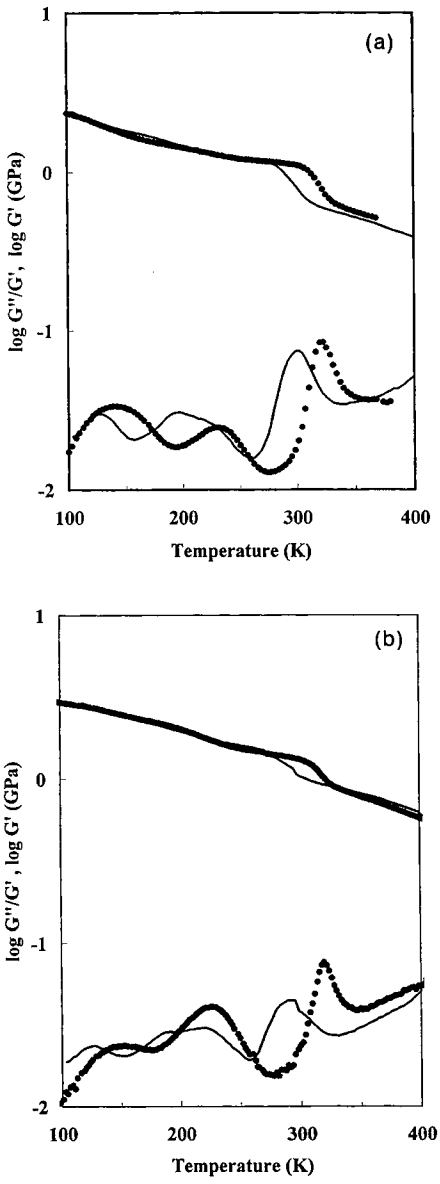

Figure 11 (●) Experimental thermograms and (——) calculated thermograms from the percolation model for the dynamic mechanical behavior at 0.1 Hz of (a) 50/50, (b) 65/35, and (c) 80/20 blends precipitated in methanol.

blends precipitated in methanol the compositions used for calculation correspond to the initial ones, which could have been affected during the precipitation step.

The more significant shift of the α tan ϕ peak for the blends precipitated in methanol could have originated from two effects: (i) the dissolution of a fraction of polyamide, essentially the lower molecular weight chains, in the methanol during the precipitation step. This last effect could result in the vanishing of the low-temperature side of the α relaxation

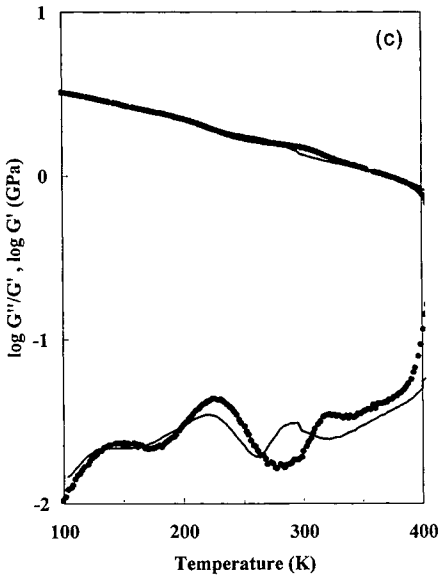

Figure 11 (*Continued*)

process, but is not sufficient to explain the shift of all the peaks, and (ii) a better miscibility between the two parent polymers, which could be enhanced by methanol. This miscibility could, in turn, lead to stronger interactions between cellulose and polyamide at the molecular level, as displayed previously in the secondary relaxation zone.

Tensile Tests

Dynamic mechanical measurements discussed above have displayed a partial miscibility between both

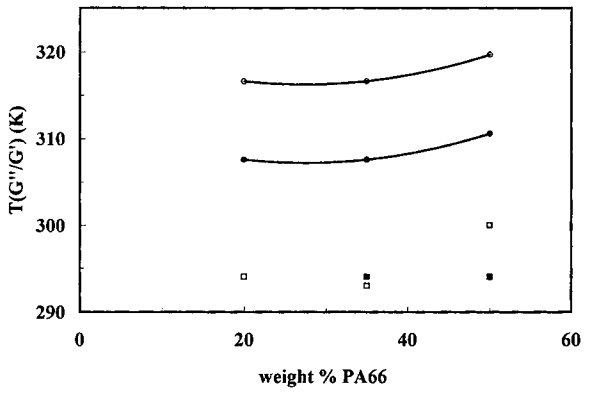

Figure 12 Temperature $T_{G''/G'}$ at the maximum of the internal friction coefficient (tan ϕ) vs. PA669 content. Experimental data of $T_{G''/G'}$ for blends precipitated (●) in water and (○) in methanol as well as calculated values for blends precipitated (■) in water and (□) in methanol are reported.

homopolymers in the blends. Assuming this point, one wonders whether this miscibility leads to a strong adhesion between phases. Tensile tests can provide an answer to this question. Stress vs. strain curves at room temperature for blends 80/20 and 50/50, precipitated either in methanol or water, are reported in Figure 13. These materials exhibit a classical behavior, i.e., a linear behavior for strain smaller than 0.02 and a decrease of the slope $d\sigma/d\varepsilon$ vs. increasing ε. The slope in the vicinity of $\sigma = \varepsilon = 0$, i.e., determined for $\varepsilon < 1\%$, is equal to the tensile modulus (E), which is known to depend on the strain rate and on temperature. Results are reported in Table IV. We ascertain that the modulus decreases as a function of polyamide content for any coagulation system. For a given composition, a higher tensile modulus is reported for materials precipitated in methanol. This is a direct indication of stronger adhesion between cellulose and polyamide. This result is also displayed through the elongation at break, which is always higher for materials precipitated in methanol than in water.

CONCLUSION

All the results obtained on the cellulose/PA669 blends exhibit a partial miscibility between both polymers, essentially when they are precipitated in methanol. This miscibility is displayed by a slight increase of the glass transition temperature of the polyamide-rich phase and to a modification of the secondary relaxations. Nevertheless, it is noteworthy that the material characteristics are very dependent on the precipitation step. The use of methanol as coagulation system leads to a stronger adhesion between the two parent polymers, as it seems to help the interdiffusion of the two parent polymers.

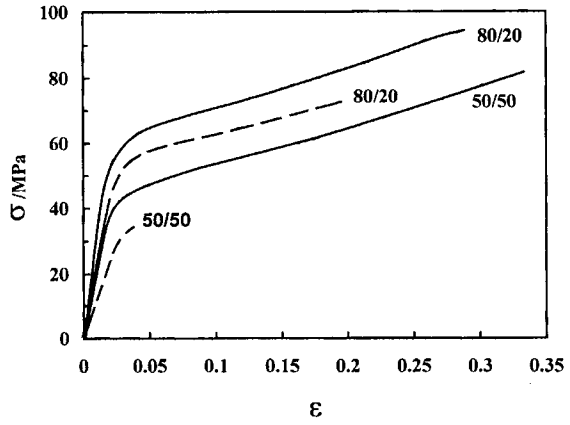

Figure 13 Stress vs. strain for blends 80/20 and 50/50 at room temperature and for $\dot{\varepsilon} = 1.7 \cdot 10^{-3}\ s^{-1}$; (——) refers to blends precipitated in methanol; (– –) refers to blends precipitated in water.

Table IV Tensile Modulus of the Various Samples

	E (GPa) Coagulation System	
Sample	Water	Methanol
80/20	2.3	3.4
50/50	1.3	2.1

M. G.-R. gratefully acknowledges CONACYT (Mexico) and SFERE SA (France) for their financial support and Dr. C. Bosso for the mass spectroscopy measurements.

REFERENCES

1. Y. Nishio and R. St. J. Manley, *Macromolecules,* **21,** 1270 (1988).
2. Y. Nishio, T. Takahashi, and R. St. J. Manley, *Macromolecules,* **22,** 2547 (1989).
3. J. F. Masson and R. St. J. Manley, *Macromolecules,* **24,** 6670 (1991).
4. M. Shibayama, T. Yamamoto, C.-F. Xiao, S. Sakurai, A. Hayami, and S. Nomura, *Polymer,* **32,** 6, 1010 (1991).
5. J. F. Masson and R. St. J. Manley, *Macromolecules,* **25,** 589 (1992).
6. A. H. Jolan and R. E. Prud'Homme, *J. Appl. Polym. Sci.,* **22,** 2533 (1978).
7. R. B. Seymour, E. L. Johnson, and G. A. Stahl, in *Macromolecular Solutions,* R. B. Seymour and G. A. Stahl, Eds., Pergamon Press, New York, 1982, p. 90.
8. Y. Nishio, S. K. Roy, and R. St. J. Manley, *Polymer,* **28,** 1385 (1987).
9. W. Berger, B. Morgenstern, and H. W. Kammer, in *Morphologies in Cellulose Based Blends,* J. F. Kennedy, G. O. Phillips, and P. A. Williams, Eds., Ellis Horwood, London, 1993.
10. Y. Nishio, N. Hirose, and T. Takahashi, *Polym. J.,* **21,** 4, 347 (1989).
11. Y. Nishio and R. St. J. Manley, *Polym. Eng. Sci.,* **30,** 2, 71 (1990).
12. N. E. Franks and J. K. Varga, U.S. Pat. 4,247,431 (1981).
13. N. E. Franks and J. K. Varga, U.S. Pat. 4,256,613 (1981).
14. M. Garcia-Ramirez, J. Y. Cavaillé, D. Dupeyre, and A. Péguy, in *Cellulosics: Chemical, Biochemical and Material Aspects,* 489, Ellis Horwood Series in Poly-

mer Science and Technology, Part 3, No. 71, Ellis Horwood, London, 1993, p. 489.
15. M. Garcia-Ramirez, J. Y. Cavaillé, D. Dupeyre, and A. Peguy, *J. Polym. Sci. Polym. Phys.*, **32,** 1437 (1994).
16. M. Garcia-Ramirez, J. Y. Cavaillé, A. Dufresne, and P. Tekely, *J. Polym. Sci. Polym. Phys.*, **33,** 2109–2124 (1995).
17. H. Chanzy, M. Paillet, and A. Péguy, *Polym. Commun.*, **24,** 171–172 (1986).
18. H. Chanzy, M. Paillet, and R. Hagège, *Polymer,* **31,** 400–405 (1990).
19. S. Etienne, J. Y. Cavaillé, J. Perez, R. Point, and M. Salvia, *Rev. Sci. Instrum.*, **53,** 1261 (1982).
20. J. Y. Cavaillé, M. Salvia, and P. Merzeau, *Spectra 2000,* **16,** 37 (1988).
21. H. Montès, J. Y. Cavaillé, and K. Mazeau, *J. Non-Cryst. Solids,* **172–174,** 990–995 (1994).
22. H. W. Starkweather, Jr., ACS Symposium Series 127, American Chemical Society, Washington, DC, 1980, p. 433.
23. W. P. Leung, K. H. Ho, and C. L. Choy, *J. Polym. Sci. Polym. Phys.*, **22,** 1172 (1984).
24. Z. Hashin, *J. Appl. Mechan.*, **50,** 481 (1983).
25. M. Takayanagi, S. Uemura, and S. Minami, *J. Polym. Sci. C,* **5,** 113 (1964).
26. E. H. Kerner, *Proc. Phys. Soc.*, **B69,** 808 (1956).
27. R. A. Dickie, *J. Appl. Polym. Sci.*, **17,** 45 (1973).
28. T. B. Lewis and L. E. Nielsen, *J. Appl. Polym. Sci.*, **14,** 1449 (1970).
29. C. Jourdan, J. Y. Cavaillé, and J. Perez, *Polym. Eng. Sci.*, **28,** 1318 (1988).
30. N. Ouali, J. Y. Cavaillé, and J. Perez, *Plast. Rub. Compos. Process. Appl.*, **16,** 55 (1991).
31. J. D. Ferry, *Viscoelastic Properties of Polymers,* Wiley, New York, 1980.
32. C. Jourdan, J. Y. Cavaillé, and J. Perez, *J. Polym. Sci. Polym. Phys.*, **27,** 2361 (1989).
33. P. G. de Gennes, *Scaling Concepts in Polymer Physics,* Cornell University Press, Ithaca, NY, 1979.
34. D. Stauffer, *Introduction to Percolation Theory,* Taylor and Francis, London, Philadelphia, 1985.

Received June 29, 1995
Accepted September 18, 1995